Received: Added at production | Revised: Added at production | Accepted: Added at production

DOI: xxx/xxxx

ORIGINAL RESEARCH PAPER

Power Flow Control in a Modular Converter With Energy Storage

Krister Leonart Haugen[1,2] | **Konstantinos Papastergiou**[2] | **Dimosthenis Peftitsis**[1]

[1]Department of Electric Energy, Norwegian University of Science and Technology (NTNU), NO-7491 Trondheim, Norway

[2]Power Converters Group, European Organisation for Nuclear Research (CERN), 1211 Geneva 23, Switzerland

Correspondence
Corresponding author Dimosthenis Peftitsis.
Email: dimosthenis.peftitsis@ntnu.no

Abstract

Using modularized power converters with scalable energy storage in particle accelerators can be further enhanced with controls that can be adapted to optimise different design targets, such as to minimise the front-end stage peak current, the depth of discharge of electrolytic capacitors or the thermal cycling of semiconductors. This paper proposes a control system that is able to individually adjust the power flow of the converter modules under pre-defined load profiles, and hence separates the use of energy storage and grid connection even under rapid cycling. The paper briefly summarises the characteristics of the modular converter and proposes four energy control strategies that have been validated by simulation as well as experimentally on a 800 kW full scale prototype. It is shown that applying each strategy, the corresponding design objectives can be achieved, for example, optimal utilisation of the energy storage systems or minimised current stress in the semiconductors.

KEYWORDS
AC-DC converters, Adaptive control, Energy balance control, Modular converter, Pulsed power supplies, Scalability.

1 | INTRODUCTION

Modularisation is currently an emerging trend in the design of modern power electronic converters[1–3]. Modularised converters exhibit many benefits, in terms of redundancy under fault conditions, parallel connection to reduce losses, standardisation etc. They can also incorporate storage in order to improve the voltage quality and stability of grids[4,5] and this is a key requirement to ensure successful integration of renewable energy sources into the grid[6].

The storage component can be any type of electrical energy storage, such as batteries, capacitors, mechanical flywheel[7,8] or supercapacitors, depending on the amount of stored energy required, delivered power and storage time[9]. Other works[10] demonstrated the use of inductive storage in conjunction with battery storage, to compensate for the difference in power demand and supply from a wind farm. Significant work has been done on modular multilevel converters (MMC) to control and manage the energy stored in the cells with the additional constraint of balancing the capacitor voltages of different cells.[11–14].

All of the converters discussed in the aforementioned literature are designed to be flexible, have high peak-power and be scalable. Such scalable solutions are also popular as renewable energy interconnectors with grid-forming requirements and integrated storage[6,15–18] or in railway application with similar bi-directional power flow requirements[19].

In the niche application of power supply for particle accelerators, reliable powering and energy efficiency are increasingly important. In particular, recycling and reusing of the magnetic field energy stored the accelerator's electromagnets has given significant energy savings in the past[20].

More specifically, DC/DC converters are used for the precise regulation of the current supplying electromagnets in high-energy physics experiments[21,22]. These electromagnets are operated in a repetitive manner[20], which results in a cycling power flow, shown in Fig. 1 and this leads to technical challenges that have been discussed in[23]. In certain applications the load mission profile is unknown[24], while at CERN, the European Organisation for Nuclear Research, the powering requirements of electromagnets are often well defined, and the designer can take this into account for optimising electrical and thermal performance of the converters.

Furthermore, in modular converters the energy recovery in storage bricks requires a topology with 4-quadrant operating capability to handle the bidirectional power flow. The topics of control[2,3,25,26] and power flow[27–30] of DC-DC converters have been extensively discussed in the literature. The authors of[31] propose a control of a converter optimised for multiple parameters simultaneously, conceived for a non-cycling application. The present work focuses on the challenge of power flow control for cycling power converters

Abbreviations: MMC, modular multilevel converter; SiC, Silicon Carbide; MOSFET, metal oxide semiconductor field-effect transistors.

comprised of different modules namely the grid-connected and energy storing bricks.

The scalability advantage of DC-DC converters for highly inductive loads has been investigated before, both with [32] and without [22] energy storage. The authors presented a first work [32] where they proposed and validated the use of two different types of voltage source bricks (i.e., one grid-connected and one energy-storing brick) operating complementary one to another in a single power converter. The purpose of that work was to demonstrate the design of power converters composed of a number of bricks (i.e., fundamental modules) that provide just the right mix of RMS input ratings and energy recovering capability when operating with an agnostic mission profile. The resulting modular converter was a first step to minimise costs for a 350 circuit project for a new experimental zone at CERN called North Area.

Considering the foundation set in the work [32], an opportunity emerge on exploiting further the cost optimization (or cost related aspects such as the lifetime, energy storage usage and peak current capabilities) by applying a modified current reference to each brick. This, particularly, exhibits advantages in the case that the mission profile is known in advance, which is common in the field of application. The authors presented simulation results of four energy management strategies in [27] that satisfy peak-shaving, optimum storage utilisation, or thermal stress objectives.

The contribution of the present paper is to demonstrate a more detailed theoretical analysis of the four strategies, the software modifications of the controller for their implementation and most importantly the experimental validation of the four strategies in a full-scale power converter prototype rated at 800 kW. Moreover, the paper presents a critical analysis of the results and their implications on the practical converter's design and operation.

The paper is organised as follows. Section 2 presents the operating constraints and load requirements for such a converter. Then in Section 3 the concept for this modular converter is briefly presented. In Section 4 the adaptive control strategy is analysed and the different optimisation strategies are explained. Section 6 shows the laboratory prototype and experimental validation of the proposed scheme. Finally, the conclusions of this work are summarised in Section 7.

2 | OPERATING CONSTRAINTS AND LOAD REQUIREMENTS

Typical magnet waveforms encountered in the transfer lines in particle accelerators are shown in Fig. 1. The different magnet loads across the length of an accelerator vary considerably in inductive and resistive values. For one single experimental area the range of current required varies between 100 A to 2 kA, hence the benefit of having a flexible converter design emerges [32,33]. In addition, during the ramp down phase of the current, there is a potential to have a negative power flow, i.e. a fraction of the energy can be recovered and used in the next cycle, which is very beneficially from an energy consumption perspective [20]. Hence, the ultimate control goal of an electromagnet is to supply it with a high-precision current, by utilizing the power converters' built-in energy storage for energy recovery at every operating cycle.

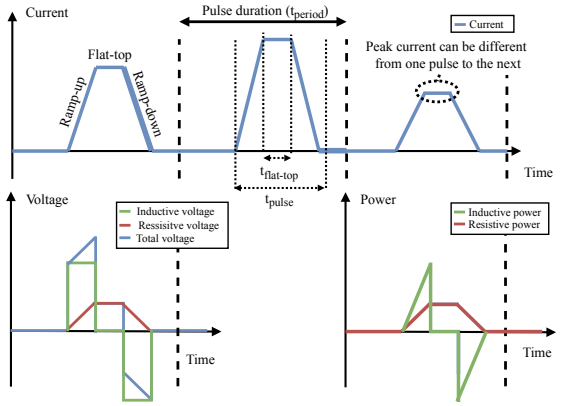

FIGURE 1 Typical current cycle sequence, dotted lines indicate division between cycles. t_{period} is typically 1.2 s, $t_{flat-top}$ is typically 50 ms and t_{pulse} can vary from 300 ms-800 ms depending on the load and flat-top current.

The maximum value of energy stored in the electromagnet field, E_{magnet} is given by Eq. 1, where L_{magnet} is the inductance of a particular electromagnet and I_{magnet} is the current through the magnet at any given time.

$$E_{magnet} = \frac{1}{2} L_{magnet} I_{magnet}^2 \tag{1}$$

By integrating adequate energy storage (e.g. capacitors) in the system, and with the power capability to deliver this energy in the relatively short time (<1 s) of the current ramp-up and ramp-down processes, the stored energy can be reused.

Since the voltage and the rate of change of voltage, dV/dt, that can be applied to the magnets are limited by design, there are limitations on how fast the current can be ramped. This voltage is often considered as a ramping voltage, shown as inductive voltage in Fig.1. The load voltage constraint determines the power converter output requirements.

3 | FUNDAMENTAL BRICK CONCEPT

This paper is based on the converter design and operation published by the authors in [33], where a more detailed description of the function and control are shown. The proposed power converter topology comprises two types of power modules or bricks; one or more *storage bricks* handle the magnetic field energy recovery while

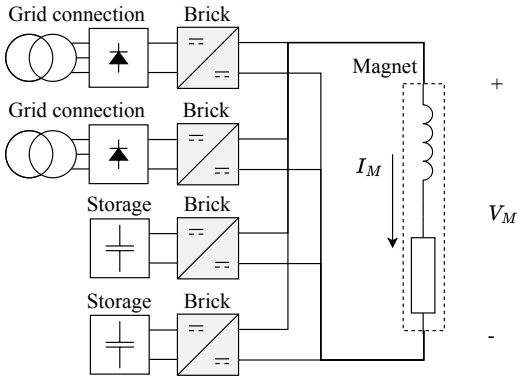

FIGURE 2 Schematic diagram showing of grid bricks and storage bricks can be combined in parallel connection of bricks. The fundamental brick in the grey box contains a full-bridge circuit with an arm inductor.

one or more *grid bricks* supply the resistive losses of the load. Each of these bricks have a certain output current and voltage capability, so the number of bricks required to meet the converter's capabilities will depend on the load requirements. As discussed in Section 2, the required currents span over a wide range and the ability to easily connect bricks in parallel makes it possible to scale the current. The required voltage for the electromagnets also spans in a wide range, which impose the need for connecting bricks in series.

The proposed structure (an example can be seen in Fig. 2), enables a converter design where the resistive and inductive power can be scaled independently. An investigation of the optimal output characteristics of these bricks has been presented in [33], such that the converter can be scaled to each magnet in an optimal way.

Each one of the grid and storage bricks is implemented using a full-bridge output stage [26,34–36] with a brick inductance L_{HF} which allows the output voltage to be independently controlled.

3.1 | Storage brick

The storage brick has the primary task of supplying the inductive power flow of the load. It features no grid-connection, and thus its operation relies on a controller that manages balanced supply and recovery of energy during each of the load cycles (in particular during the ramp-up and the ramp-down of the current). The ramp-down phase is described in Fig. 1. The storage brick will connect to the load using the fundamental brick described above, and will store energy using electrolytic capacitors connected to a DC-bus on the input side of the full-bridge in the fundamental brick.

Since the peak power by these converters is only delivered during ramp-up and ramp-down, the storage components need to deliver the majority of their energy in less than one second. Thus, capacitors have been chosen as appropriate storage elements [37]. This, in turn, means that the bus voltage in the storage bricks depends on the state-of-charge of the storage capacitors. In order to maximise the utilisation of the capacitors, the nominal bus voltage has been chosen to be the highest voltage the power semiconductor devices can safely manage.

The storage capacitors and the nominal voltage determine the amount of energy stored in the storage bricks. Given the need to use H-bridges to supply the magnets, it is only possible to step down the voltage from the DC bus. This limits the lowest voltage the storage bus can accept, since there has to be sufficient voltage left on the bus to deliver the full output voltage.

The minimum requirement for the voltage on the capacitors reduces the amount of usable energy in the capacitors. Eq. 2 expresses the usable energy in the storage brick, E_{brick}, as a function of the capacitance of the storage brick, C_{str}, nominal DC-bus voltage, V_{bus} and the lowest allowable voltage on the bus, V_{out}, in order to deliver the required output voltage for the brick.

$$E_{brick} = \frac{1}{2} C_{str}(V_{bus}^2 - V_{out}^2) \tag{2}$$

This is where the complexity of designing the storage bricks emerges. If the output voltage is selected to be relatively high, then the usable energy in the capacitors is somewhat limited for a given capacitance in the storage bricks. This implies that either a large number of storage bricks is needed to achieve the required storage for supplying the inductive stored energy in the magnet, which increases the cost of semiconductors and capacitors; or that each storage brick needs a large number of capacitors, making them more costly and storing more energy, increasing the short-circuit energy. However, if the output voltage is selected to be relatively low, then the storage capacitors are utilised at a larger degree, and fewer capacitors are needed overall to satisfy the storage requirements. In this design scenario, the number of bricks starts to increase, in order to achieve the voltage requirement of the individual magnet. This trade-off has been discussed in detail in a previous publication and based on the findings there [33], a brick size of 200V and 400A has been specified.

3.2 | Grid brick

The grid bricks will use the same bus and output voltage as the storage bricks. This is the condition to ensure re-usability of the design and components. Since the grid bricks in principle only need to supply the power losses in the magnet, there is no need to consider bi-directional power flow or the state-of-charge of the storage, making it a more simple component to scale. The grid brick is supplied by a diode rectifier connected to a three-phase AC grid, hence no power shall ever flow back to the grid.

While the grid bricks and storage bricks could be dimensioned in terms of voltage ratings independently, for the sake of standardisation and to allow the bricks to be freely connected in series and parallel, the output voltage of the grid bricks was chosen to be the same as for the storage bricks.

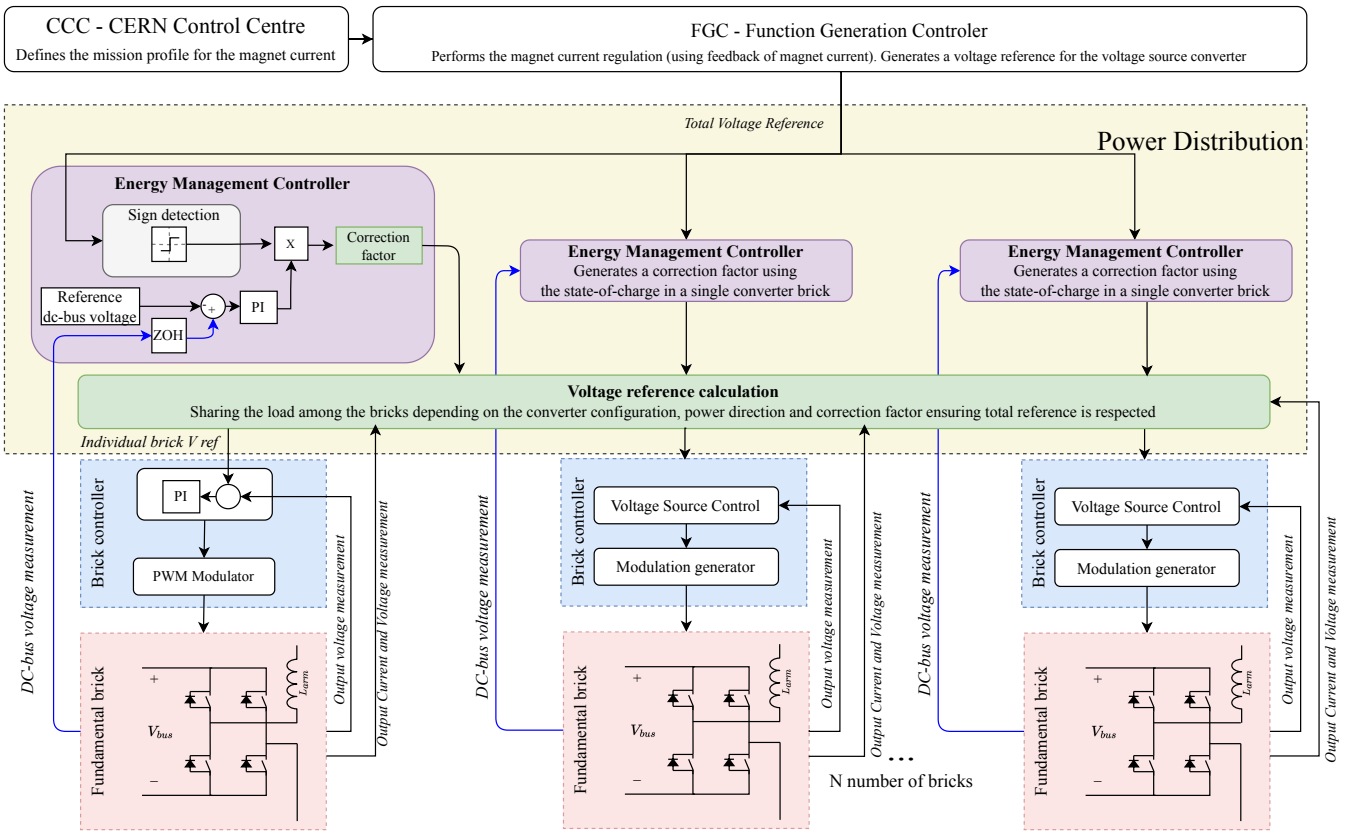

FIGURE 3 High level controller of the converters at CERN. The proposed energy controller that inserted in the control chain is shown in the yellow shaded area.

4 | POWER FLOW CONTROL IMPLEMENTATION

This section presents a brief overview of the typical control structure for the power converters at CERN (Fig. 3). This control structure is used as the foundation to develop the four proposed power flow control strategies that are presented in this paper.

The scalable converter is controlled by a central energy controller. This controller is responsible for distributing the energy flow between the grid-connected and the energy-storage bricks of the converter. The primary target is to respect the total voltage and current references and to ensure that the energy in the storage bricks are maintained at the desired level. A principle sketch of the controller structure of the converter used in this paper is shown in Fig. 3, the yellow shaded area shows where the code is inserted into the existing control structure. The controller uses the storage state-of-charge information and regulates the power flow between the bricks to maintain the state-of-charge at the end of each supplied pulse, taking advantage of the power supplied to the load and circulating currents to replenish the storage.

While the primary targets poses some limitations on the range of operation, there is normally still quite a lot of room left to have a secondary target. This is used in this paper to optimise for different targets such as to limit the grid-current, to increase the usage of the storage, or to achieve a certain regulation precision in the output current. By regulating the power flow, the controller adjusts the peak and RMS current loading of each brick. Additionally, the power flow among different bricks may be optimised for smaller temperature variations of the power semiconductors modules and thus, improving their expected lifetime.

The configuration discussed in this work is four parallel-connected bricks; two of them are storage bricks connected to capacitive energy storage and two of them are grid bricks connected to the power grid.

When a higher voltage is required to supply the load, the bricks need to be connected in series, but the principle of distributing the power supplied by the different bricks remains. This approach is made easier by the fact that the current can be considered the same for all series connected bricks, and the voltage of the individual bricks regulated to supply the desired power. The function generation controller (FGC) acts as the system controller, receiving the mission profile from the CERN Control Centre and controlling the current at the load level. The reference is then passed on to the energy regulator in the converter, which regulates the bus voltage in the storage bricks by calculating the energy available and dispatching a modified current reference for each of the bricks independently.

The calculation depends on the configuration on the bricks in the converter. If all bricks are connected in parallel, then the output voltage is necessarily always the same, but the energy management controller can distribute the current between the bricks, while always respecting the total current. This modifies the reference given to the voltage loops in the individual bricks, using the added inductance in each brick to regulate the current. If the bricks are connected in series, the voltage to each brick can be controlled more directly, but the energy management controller must take the current into account in order to correctly anticipate the delivered and recovered energy. The theoretical background for this implementation strategy has been presented in [27], including the redistribution of power flow during a fault condition.

5 | GRID CURRENT CONTROL STRATEGIES

In a conventional converter topology with four parallel connected bricks, all of them receive the same trapezoidal current reference and supply equal parts of the total current (this reference is represented with a grey colour line in the graphs of Fig. 4). The proposed control scheme produces different reference shapes for the grid bricks to satisfy different objectives as discussed in [27]. Key waveforms are reported in this paragraph to provide the necessary context for the laboratory verification in the following section.

It is reminded that the role of a grid-connected brick is to supply the losses in the magnet and the system. Besides, it should be noticed that the current contributed by grid bricks may exhibit negative values in the ramp-down phase (red, pink and green curves in Fig. 4). This negative current, and the corresponding negative voltage delivered by the brick, are necessary to keep a positive power flow during the ramp-down phase for the grid brick.

Each control strategy provides a different current reference for the grid current. The grid current reference is calculated by considering the goal of the specific strategy, as well as a number of design and operating parameters of the scalable converter. Considering the overall structure of the controller (Fig. 3), the grid current references are calculated in the green box in Fig. 3. Table 1 summarizes the key objectives of the different strategies.

The storage brick current references are then calculated to ensure that the total magnet current reference is respected, and some checks are done to ensure the maximum allowable current for the bricks is also respected. It should be noted that the total current control is performed by the FGC exclusively. The controller is utilising measured values for the magnet current and voltage, to overcome limitations in the control structure. The output of the Energy Management Controller (C_{PI}), the purple box in Fig. 3, is updated only after every cycle to avoid stability issues in the controller. The initial value of C_{PI} has to be calculated in each case to account for the magnet current profile, resistance and inductance. The PI-controller is then able to compensate for unbalances in the capacitance on the DC-bus, losses due to parasitic resistance in the cables and losses in the switches. In the case where the load is purely resistive, the value of C_{PI} is equal to 1 for Strategy 1 and 2 and equal to the magnet current RMS in Strategy 3 and the magnet instantaneous losses in Strategy 4.

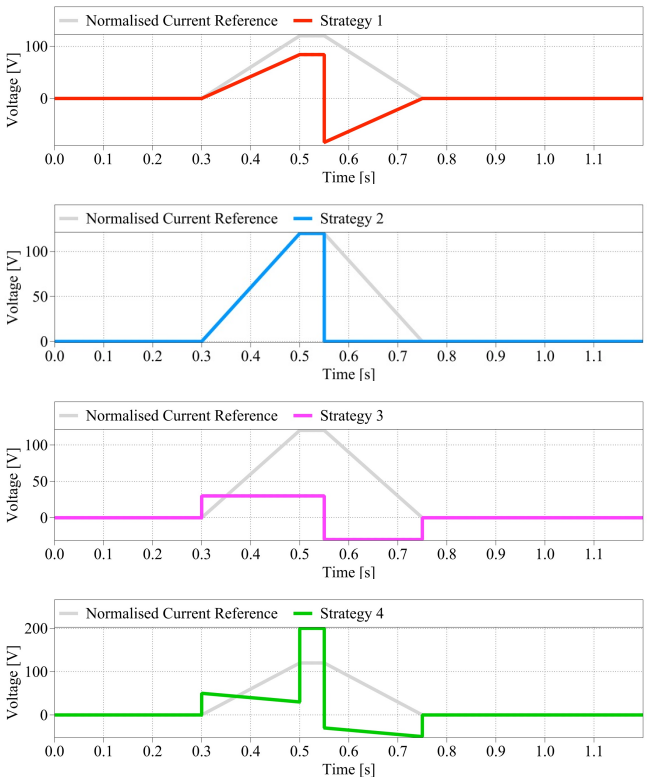

FIGURE 4 Possible grid brick reference shapes for the implementation of the different energy management strategies described in Section IV.

Strategy	Current stress sharing	Grid load	Storage utilisation	Stability
1	✓			
2	✓			✓
3		✓	✓	✓
4		✓	✓	

TABLE 1 Summary of key objectives for each control strategy used in the green box in Fig. 3.

Figure 4 illustrates the modified current reference shapes generated for the grid brick by the proposed controller. The four control strategies and corresponding current shapes in this figure are discussed in detail in the following paragraphs.

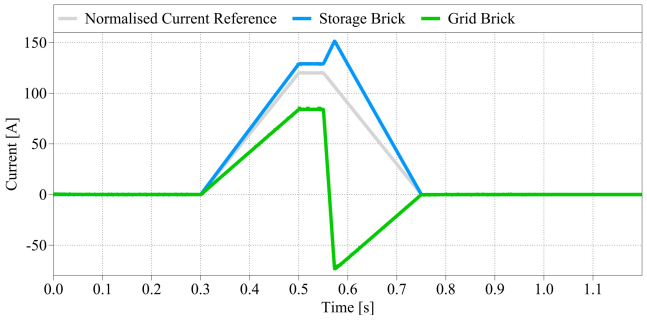

FIGURE 5 Simulation results showing the normalised output current (grey line), the grid brick current (green line) and the resulting storage brick current (blue line) by applying Strategy 1. This strategy results in a balanced RMS loading among converter bricks.

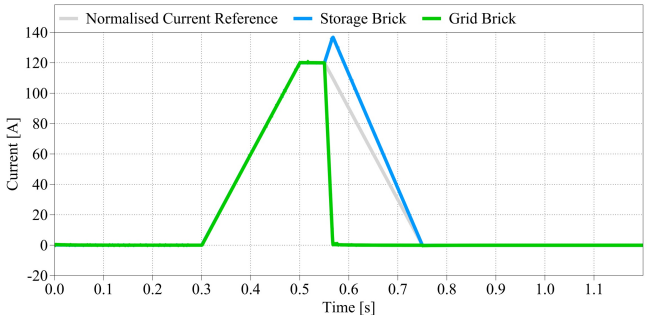

FIGURE 6 Simulation results showing the normalised output current (grey line), the grid brick (green line) using the short trapezoidal current reference and the storage brick current (blue line) by applying Strategy 2.

5.1 | Strategy 1: Current sharing among bricks

The objective of this control strategy is to ensure that the storage and grid bricks provide relatively balanced power to the load. The current reference of the storage brick is illustrated with a blue line in Fig. 5. The strategy often yields optimal current sharing among the bricks when the (recoverable) magnetic energy is comparable with the thermal losses of the inductive load during a cycle.

In the simulated example, this strategy results in a higher peak current for the storage brick, which reaches 150 A for a short duration at the start of the ramp down. This is a consequence of the reversal of the grid brick current taking place during ramp down; its current reference is governed by Eq.(3) where I_{mag} is the measured current of the electromagnet, C_{PI} is the output of the energy management PI controller, N_{grid} is the number of grid bricks and P_{dir} is the direction of power flow (either 1 or -1).

$$I_{grid,ref} = I_{mag} C_{PI} \frac{P_{dir}}{N_{grid}} \tag{3}$$

A negative power direction (the load returns its stored energy) will result in a negative grid current as soon as the ramp down starts. The current spike magnitude, illustrated by the blue line in Fig. 5, depends on the specific load and current sharing between the two types of bricks and imposes peak current requirements on the storage brick. However, it does allow the grid brick to supply power during the entire current pulse, hence a balanced RMS current sharing among bricks.

5.2 | Strategy 2: Sharing current stress among bricks - without current reversal

This strategy forces the brick to deliver the required storage in a shorter time, since it cannot contribute during ramp-down, resulting in a higher current during the ramp-up and flat-top of the pulse shown in Fig. 6 while it imposes an always positive current to be supplied by the grid bricks, unlike with Strategy 1.

In this case, the grid does not supply any power during ramp-down, which saves the grid bricks from having to reverse their current direction. This enhances voltage stability as it avoids large current gradients. It should be noted that the grid bricks can be conceived as single-quadrant in this case, since they never recover energy, also allowing a smaller DC-link capacitor to be used.

It can be noted that the action of the storage and grid bricks is very similar while each of the bricks is taking care of its respective mission; storage bricks recover the total load energy and grid-bricks provide only RMS power. Since the grid brick has a shorter time to supply the losses occurring in a cycle, it has to supply a higher peak power than the previous current shape strategy.

The grid current reference for Strategy 2 is expressed as shown in Eq. (4), where I_{mag} is the measured current of the electromagnet, C_{PI} is the output of the energy management PI controller, P_{dir} is the direction of power flow (either 1 or -1) and N_{grid} is the number of grid bricks.

$$\begin{aligned} I_{grid,ref} &= I_{mag} C_{PI} \frac{P_{dir}}{N_{grid}} | P_{dir} = 1 \\ I_{grid,ref} &= 0 | P_{dir} = -1 \end{aligned} \tag{4}$$

5.3 | Strategy 3: Minimal grid peak current

The objective of this strategy is to perform grid current peak-shaving by employing the energy storage to supply load current peaks. To achieve the objective the grid current reference is fixed as given by the governing Eq. (5), where C_{PI} is the output of the energy management PI controller, P_{dir} is the direction of power flow (either 1 or -1) and N_{grid} is the number of grid bricks.

$$I_{grid,ref} = C_{PI} \frac{P_{dir}}{N_{grid}} \tag{5}$$

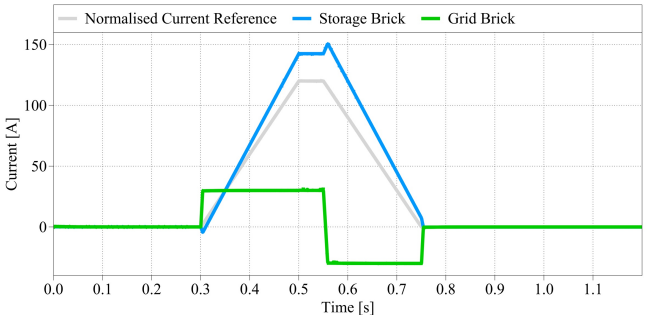

FIGURE 7 Simulation results showing the output current, the grid brick using the constant current reference (Strategy 3).

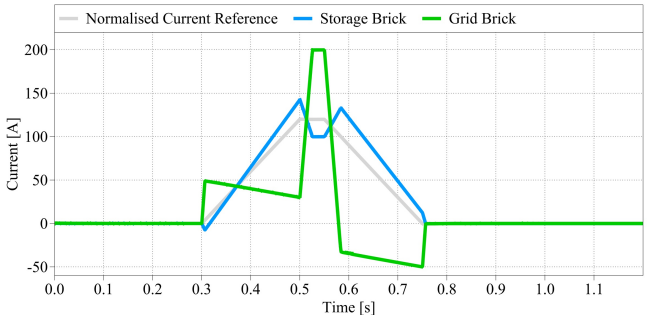

FIGURE 8 Simulation results showing the output current, the grid brick using the approximated constant power current reference (Strategy 4).

Fig. 7 shows typical simulation results for the currents when Strategy 3 is applied. As can be observed, the current of the grid brick is larger than the magnet load current at the beginning of the pulse. Hence, it becomes apparent that under this operating mode, the storage bricks must reverse their current direction, and also increasing the voltage on the storage above the nominal value. For a magnet exhibiting higher losses, the grid current will be relatively higher, and the increase of the bus voltage at the beginning of the pulse will be more significant.

Strategy 3 utilises most of the installed storage in the scalable converter. This is due to the fact that the peak values of the grid-bricks current are lower than in the other strategies. Hence, the storage bricks supply a larger amount of current during the flat-top period of the pulse. In case that a long flat-top duration red is required, a significant limitation emerges; supplying a magnet with current from a capacitor bank requires very large energy storage capability, which eventually increases the installation cost of the converter.

5.4 | Strategy 4: Minimal peak grid power

The objective of the last strategy is to provide a constant power from the grid; the current reference is estimated based on an approximation of constant power dictated by the voltage on the magnet, as shown in Eq. (6), where C_{PI} is the output of the energy management PI controller, N_{grid} is the number of grid bricks and V_{mag} is the measured voltage on the load. With this strategy, the storage bricks supply the majority of the power during flat-top, which implies maximum utilisation of the energy storing units. Moreover, this strategy enables minimisation of the front-end power requirements at the cost of larger storage requirements and higher power losses in the storage bricks. Similarly to Strategy 3, here the storage bricks have to absorb energy and reverse their current direction during the first instants of the pulse. The current direction changes require the current regulators of each brick to adjust the dI/dt in a manner contrary to the global (load) dI/dt. This can result in control instabilities if the cascaded loop dynamics are not decoupled.

$$I_{grid,ref} = C_{PI} \frac{1}{V_{mag} N_{grid}} \tag{6}$$

Figure 8 shows simulation results when applying Strategy 4. In this figure, the green line presents the output current from the grid brick. It is observed that the grid brick current rate changes significantly several times during the period of the pulse. During the flat-top interval, the grid current has a very high value, while during the ramp-down phase this current reverses into a negative value. As a result, a power dip in the supplied power from the grid brick occurs, and the storage bricks compensate the difference. Strategy 4 is generally beneficial for the converter's performance in the case where the magnet's power losses are larger than the stored energy in the capacitors or where the pulses are much longer. However, this also worsens the issue with a negative current for the storage bricks at the start of the cycle. A possible solution to this is to develop a hybrid approach, where the current amplitude is continuously limited to below the magnet's current in order to eliminate reverse currents in the storage bricks. Nevertheless, such an approach would approximate the minimal grid RMS current approach (Strategy 3).

6 | LABORATORY EXPERIMENTAL RESULTS

For the experimental validation, an existing 800 kW power converter in the CERN laboratory was used. Typically, the existing power converters at CERN feed power to the electromagnets using an H-bridge circuit that is supplied by the grid through a low-frequency transformer, a diode rectifier, a DC/DC boost converter and a capacitive bank. The power converter used for the experimental validation contains two grid bricks and two storage bricks. For realizing the hardware of the storage bricks, the transformer and diode rectifier have been disconnected and the storage bricks have a large capacitor bank used for the energy storage. On the other hand, the grid bricks' hardware configuration is kept as in the existing

converter. In particular, the grid bricks are supplied from the electrical grid via a transformer, a diode rectifier and a DC/DC boost converter stage. This enables the grid brick to supply the losses of the grid bricks, storage bricks and the losses in the load. The storage bricks are designed to supply power as long as the voltage is between 600 V and 900 V, and the corresponding usable energy can be calculated from Eq. 2 and is 13.5 kJ per storage brick. A photograph of the test setup is included in Figs. 9 and 10, with the schematics of the topologies shown in Fig. 11. The grid bricks are brick A and B, and the storage bricks are brick C and D.

TABLE 2 Converter IGBT parameters

CM1200DC-34N	Voltage	Current
Rated value	1700 V	1200 A
Max designed	450 V	450 A

The converter is controlled by a Texas Instrument DSP. It is integrated with a CERN developed current measurement system and uses LEM sensors for voltage measurements (LV 25-P/SP5 both on the output and the DC-bus). The CERN developed current measurement system (DCCT) has the ability to measure current with a significant accuracy in the parts-per-million (ppm) range. With the parameter of the IGBT used listed in Table 2, it is clear that these devices are significantly de-rated in their designed operation. This is to achieve lifetime requirements due to the thermal impact of cycling loads.

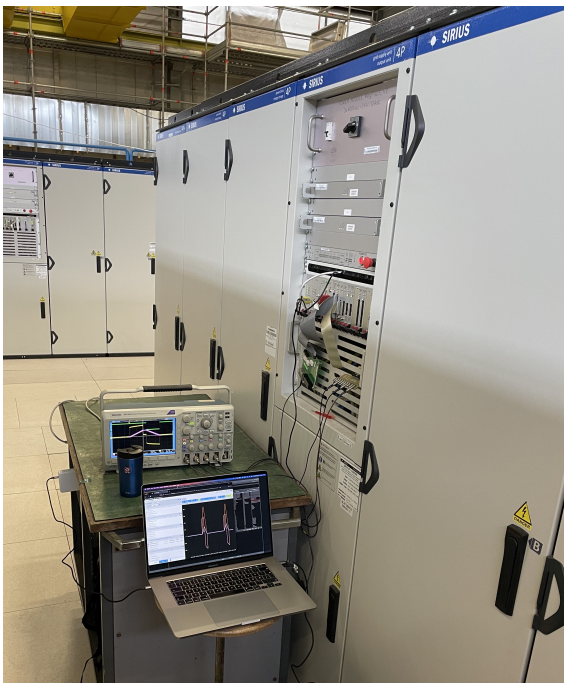

FIGURE 9 Photograph of the laboratory setup.

TABLE 3 Converter parameters

	Grid Connected Brick	Energy Storage Brick
Max Voltage	200 V	200 V
Max Current	450 A	450 A
Energy Available	N/A	56.4 kJ @900 V

FIGURE 10 Photograph of the laboratory setup, showing the power stack, gate drivers and DC-bus filter capacitors integrated into the cabinet. The storage capacitors can be seen at the bottom.

As mentioned above, the existing converter, used in the CERN East Experimental Area[20] been modified as illustrated in Fig. 11 by disconnecting the grid connection (via a transformer, a diode rectifier and a DC/DC boost converter) of two out of four bricks. The converter parameters used by the converter in the test setup are summarised in Table 3. With the connection to the grid disconnected, the storage bricks are simply a full-bridge converter switching at 6.5 kHz with a large capacitive dc-link connected on the front. A minimum of capacitors on the grid bricks are kept to form the necessary dc-link. Since the storage bricks do not have their own source of energy, the grid bricks shall supply the losses for the complete system, as well as for the load. By separating the grid connection and storage, it is possible to scale the converter for storage and grid connection independently, and by using the same brick to connect to the load, the system complexity is kept to a minimum. The prototype hardware is based on well-designed converters whose feasibility -including protection functionalities- has been proven in the field. Thus, to demonstrate the feasibility and performance of the proposed power flow control strategies, parts of the controller shown in Fig. 3 have been modified. At the same time, it was assured that the existing output performance of the converter is maintained.

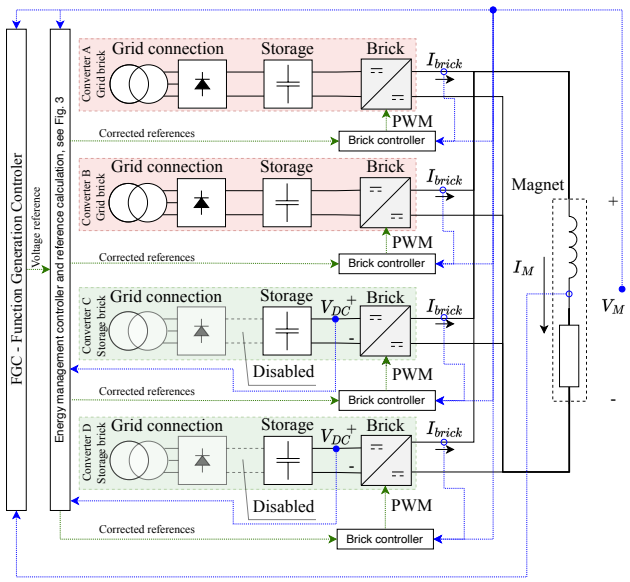

FIGURE 11 Schematic diagram of the converter topology used in the lab setup and configured with two grid and two storage bricks, only one set of measurement signals shown. The shaded area illustrates the hardware that is removed as a result of the proposed control scheme.

TABLE 4 Parameters of the load used for the experimental setup

Load parameter	Value
Inductance	430 mH
Resistance	83 mΩ
Max current	916 A
Pulse current flat-top	700 A
Peak stored energy at @700 A	105.35 kJ
RMS power	8 kW
Peak power	175 kW

The load used in this paper is four parallel-connected accelerator electromagnets with solid iron core that are commonly used in accelerator facilities. Its key parameters are listed in Table 4.

6.1 | Strategy 1

Using the strategy described in subsection 5.1, the current sharing between the storage and grid bricks are shown in Fig. 12a. The storage bricks supply approximately 200 A (bricks C and D), during the current ramp and flattop, and recover a peak of 440 A during the ramp-down phase. It is interesting to note that when the current supplied by the grid-brick reverses the storage brick is forced to compensate with an additional equivalent current, which increases its peak current contribution. This however results in more energy recovery due to the negative output voltage during this time.

The DC-link voltage plots in Fig. 12b demonstrate the energy recovery performed by the storage bricks throughout the cycle which guarantees that enough energy will be available for the next load cycle.

A summary of the performance indicators are listed in Table 5. The storage bricks use the energy recovered during the ramp-down phase to cover the losses of the storage bricks, as well as contributing to the current delivered during ramp-up and flat-top intervals.

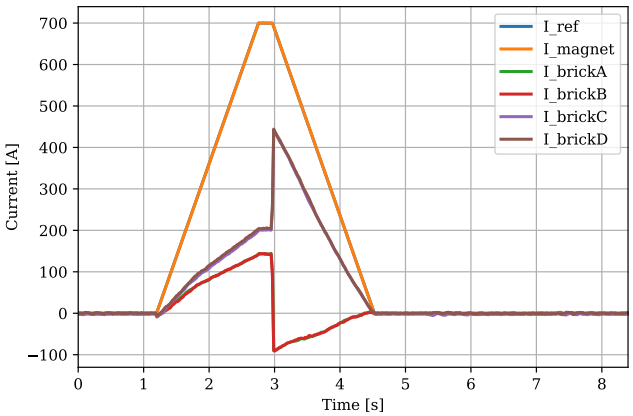

(a) Experimental measurements of the magnet and bricks currents

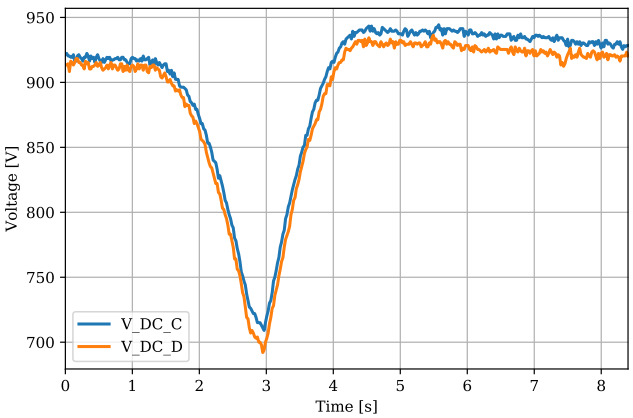

(b) Experimental measurements of the DC-dus voltages for the storage bricks V_{DC_C} and V_{DC_D}

FIGURE 12 Experimental results for Strategy 1: Sharing current stress

6.2 | Strategy 2

This strategy is similar to the previous one with the difference that the grid brick current is not allowed to reverse. As described in subsection 5.2, the grid bricks (A and B) are effectively delivering zero current during the ramp-down phase, as shown in Fig. 13a. The storage bricks (C and D) recover the totality of the energy into

the storage element. This is fairly typical for this approach, and the more energy the storage bricks can recover, the higher current they can supply during the ramp-up and flat-top of the next cycle. Again Fig. 13b shows that the energy in the storage bricks maintained at the end of the cycle; thus, the energy controller has found the optimal distribution of currents using this strategy.

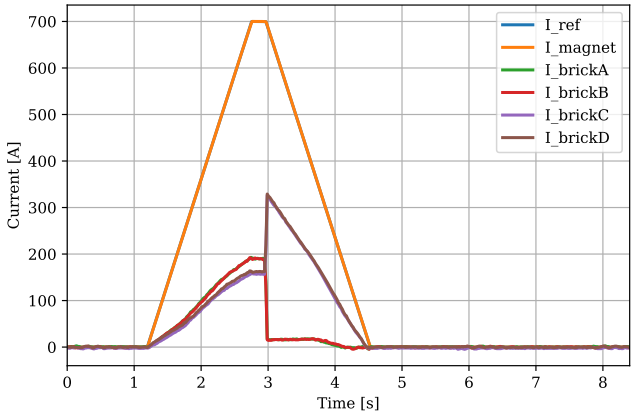

(a) Experimental measurements of the magnet and bricks currents

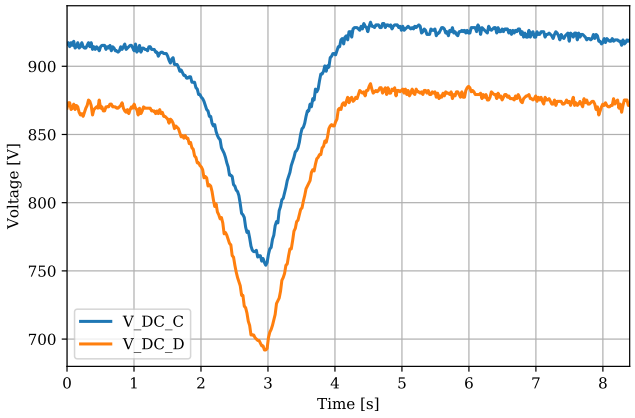

(b) Experimental measurements of the DC-dus voltages for the storage bricks V_{DC_C} and V_{DC_D}

FIGURE 13 Experimental results for Strategy 2: Sharing current stress - Short

6.3 | Strategy 3

With this strategy, as described in subsection 5.3, the grid bricks maintain a constant current during the ramp-up and flat-top, before reversing to the same negative current value during the ramp-down phase. As shown in Fig. 14a for bricks A and B, the grid bricks reach 80 A and maintain this value until the end of the flat-top. Then the current flips to -80 A to keep the power flow from the grid brick positive. The storage bricks (C and D) are left to ensure that the total current reference is respected, and the energy controller has to calculate what the current value for the grid bricks should be, shown as the green and red lines in the plot (Fig. 14a). Similarly to the cases above, it is observed that this strategy also results in the energy being conserved in Fig. 14b; notice also that the storage is used during the first 300 ms to absorb energy, enhancing the usage of the storage. The energy used and other key metrics are listed in Tab. 5.

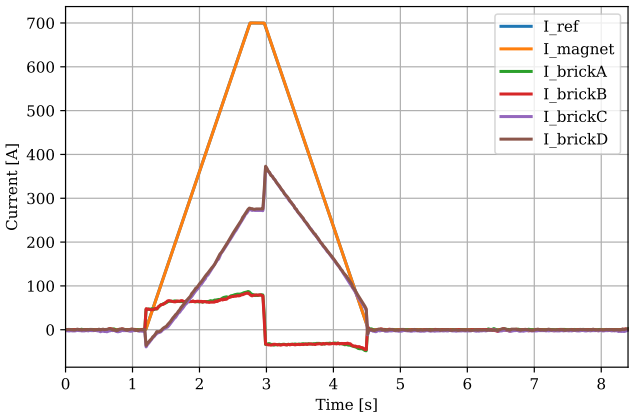

(a) Experimental measurements of the magnet and bricks currents

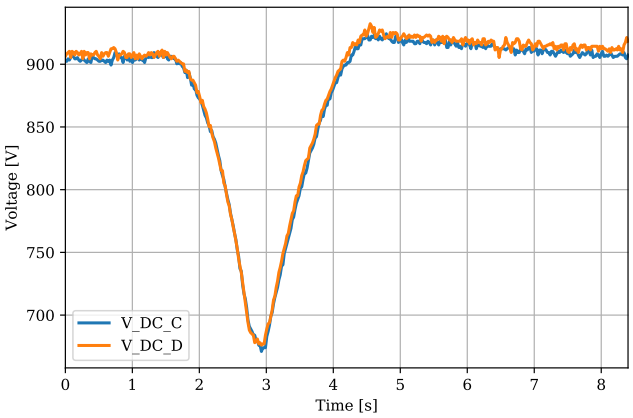

(b) Experimental measurements of the DC-dus voltages for the storage bricks V_{DC_C} and V_{DC_D}

FIGURE 14 Experimental results for Strategy 3: Minimal grid current RMS

6.4 | Strategy 4

The final strategy is also the most demanding from a regulation perspective, as described in subsection 5.4. Using Strategy 4, the current estimate is now also dependent on the load voltage, and so the references change significantly throughout the pulse. However, as shown in Fig. 15a the regulator is able to follow this varying current quite well, and the storage bricks ensure that the total current

reference is always respected. The energy regulator has found a stable grid brick power, sufficient to maintain the energy stored in the storage bricks, as illustrated in Fig. 15b.

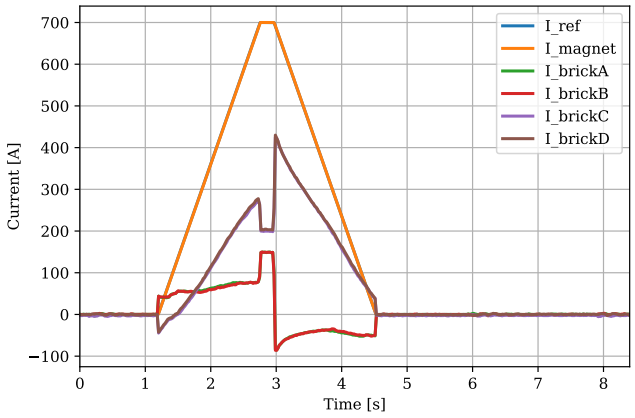

(a) Experimental measurements of the magnet and bricks currents

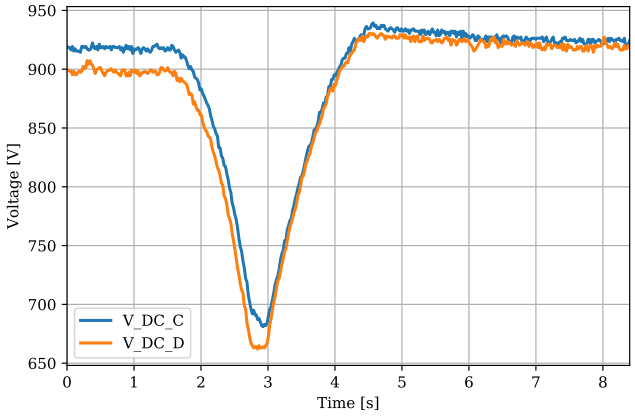

(b) Experimental measurements of the DC-dus voltages for the storage bricks V_{DC_C} and V_{DC_D}

FIGURE 15 Experimental results for Strategy 4: Minimal peak grid power

7 | DISCUSSION

The proposed scalable power converter that is built with grid bricks and storage bricks overcomes the limitations of existing power converter designs for supplying electromagnets in particle accelerators. Traditionally, power converters for these applications integrate grid and storage connections in the same DC link[21]. This poses limitations in terms of redundancy, scalability and energy control flexibility for reducing converter's electrothermal stress.

Designing a scalable and modular power converter allows the separation of grid and energy storage connections. In particular, by such a converter with two types of bricks (i.e., grid bricks and storage bricks) a more flexible operation is enabled compared to traditional technologies. Scalability is achieved by combining a certain number of grid bricks and storage bricks for fulfilling the load constraints of various electromagnets[32]. Still, to exploit the cost benefits of this scalable power converter fully, it is imperative to develop power flow control strategies, which control the energy supplied and recovered to the bricks at every cycle of operation. A comparison of the four strategies in selected and key metrics are presented in Table 5. The values presented are the averages of the two bricks of the same type. These metrics highlight the different utilisation of the converter hardware by the four strategies. The total output current and output voltage are always the same regardless of the strategies, as this is defined by the load mission profile. The way energy is dispatched by the converter bricks differs according to the control strategy. Therefore, to demonstrate the feasibility, performance and advantages of each control strategy, and to allow a fair comparison among the strategies, the design parameters of the bricks (e.g., the capacitance of the capacitive bank, power semiconductors ratings etc.) have been kept the same.

Comparing Strategies 1 and 2 in Table 5 the RMS current values are very similar between the grid brick for Strategy 1 and 2 and storage bricks for strategies 1 and 2. For Strategy 1 approximately 46.8 kJ of the energy cycled per brick, this is equivalent to 89% of the energy stored in the magnet. The storage bricks are also reaching their current limit, during the ramp-down.

While for Strategy 2 the recycled energy is slightly decreased, which indicates that such a strategy allows to reduce the amount of installed energy storage which costs approximately 250 EUR/kJ in this type of converter. The energy recovered is about 72 % of the total stored in the magnet as shown in Tab. 4, after accounting for losses this is close to the maximum which can be extracted. The other strategies uses the grid brick to inject more energy during the ramp-down, enhancing the usage of the storage. Similarly the peak current of the storage bricks is reduced leading to less thermal stress in the semiconductors, maximising the cycling lifetime of the IGBTs. Since the brick and storage bricks use the same full-bridge topology, the second strategy also leads in better utilisation of the grid-brick hardware.

Strategies 3 and 4 are primarily targeted to limiting the cycling impact on the power grid by performing some sort of peak shaving. This reduces the installed power requirement for the grid, and can also be used to limit the peak-power during high demand periods. Strategy 3 in Table 5 introduces a lower RMS current for the grid bricks, compared to strategies 1 and 2. However, there is a corresponding increase for the storage bricks usage; the storage bricks recover some energy during the ramp-up phase, as well as the ramp-down phase, and therefore have more energy available to deliver to the load. In total the storage bricks uses an amount of storage equivalent to 94% of the energy in the magnet. Achieving a reduced grid supply loading and using more energy storage, may be a useful objective in certain applications and these are candidate applications for strategies 1 and 2. However, it should be noted that

TABLE 5 Comparison of Grid brick power sharing strategies

Strategy	Key metric	Grid Brick	Storage Brick
Strategy 1	$I_{RMS-out}$	45.1 A	115.0 A
	I_{peak}	144.2 A	444.3 A
	ΔV_{bus}	-	240 V
	ΔE_{str}	-	46.8 kJ
Strategy 2	$I_{RMS-out}$	53.3 A	88.9 A
	I_{peak}	193.0 A	329.1 A
	ΔV_{bus}	-	187 V
	ΔE_{str}	-	37.7 kJ
Strategy 3	$I_{RMS-out}$	32.1 A	115.5 A
	I_{peak}	87.4 A	373.2 A
	ΔV_{bus}	-	255 V
	ΔE_{str}	-	49.3 kJ
Strategy 4	$I_{RMS-out}$	39.0 A	120.5 A
	I_{peak}	149.0 A	430.0 A
	ΔV_{bus}	-	263 V
	ΔE_{str}	-	50.6 kJ

these strategies load the two types of bricks unequally, which could result in a different lifetime of the two types of bricks (assuming identical ratings).

Finally Strategy 4 aims to reduce the peak grid power, which eventually results in a very different utilisation of the bricks. The storage bricks are carrying most of the current, and also their reference varies considerably throughout the load cycle. In total the storage bricks uses an amount of storage equivalent to 96 % of the energy in the magnet. This strategy is best served if the grid supplying the converter is limited in the available power, or increasing installed power is very costly, so that minimising the installed power requirements is beneficial. It also shows how creative it is possible to be with the currents from the different bricks, without affecting the performance with respect to the output current precision.

Ultimately, the choice of the optimal strategy is impacted by several parameters, including the flat-top duration, the L/R-ratio of the magnet load, cost of cooling and the availability/cost of front-end peak power capability. The advantage of such a modular design is that the utilised strategy can be adapted to the individual load by using the same converter topology. The energy storage or grid-connection costs can be optimised on circuit per circuit basis in a large industrial complex, by modifying the way energy is dispatched to the load.

The energy flow in the system, meaning the energy exchange among the load, the storage bricks and the grid connected bricks, is controlled by an energy controller by choosing the appropriate current reference shape for the grid brick and finding the optimal current distribution between the bricks. By having a shape which follows the current to the load, i.e., trapezoidal, the current stresses in the brick switches and losses are shared most equally among the bricks. Two additional strategies, aiming at reducing the front-end peak power have also been shown. These strategies are mostly suited for relatively short pulses in inductive loads, with a large amount of recoverable energy compared to the losses. It has been shown that it is possible to have any number of bricks connected in series and parallel, and within their current and voltage ratings, the power-flow can be individually controlled.

Since both bricks operate during most of the cycle time, the thermal cycling of semiconductors would probably be very similar. At the same time the re-circulation of energy among bricks to balance the energy, can result in higher RMS current on the bricks, thus potentially increasing the losses.

Regardless of the number of grid or storage bricks, each scalable converter supplies energy to a single electromagnet in the field at CERN complex. Therefore, the risk for unbalanced loading conditions is not present. Due to parallel-connected bricks that are required by the electromagnet loads, a risk for current unbalances might exist. However, using the proposed controller, it has been demonstrated experimentally in the full-scale power covnerter that a satisfactory current balance is achieved. Moreover, parameters variations among different electromagnet loads, that are supplied by the same scalable converter, or non-linear electromagnet properties might exist. In this case, the FGC-Function Generation Controller (Fig. 3) which contains specific functionalities, is able to compensate for any parameters variations among the different electromagnets, as well as for non-linear characteristics of these loads. However, this aspects of the FGC-Function Generation Controller were not within the scope of this paper.

As mentioned above, the H-bridge circuits employ IGBTs power modules. The voltage and current requirements for each brick, do not impose series- or parallel-connections of IGBTs modules within each brick. Thus, possible gate signal mismatches within a single H-bridge circuit are eliminated. Moreover, gate signal mismatches among the IGBTs power modules employed in different H-bridge circuits, do not pose a risk either. In particular, the switching operation of each H-bridge circuit is decoupled from each other by means of an inductor connected on the bricks' outputs.

8 | CONCLUSION

An energy flow control scheme for a modular DC/DC converter has been proposed and experimentally validated in a full-scale 800 kW prototype. It has been shown that the controller guarantees the energy balance as well as the output current regulation under rapid cycling load conditions. The 4 converter bricks deliver different currents, satisfying the power flow requirements for each strategy. In doing so each strategy fullfils an objective such as minimising the front-end (grid) current, reducing the capacitor's depth of discharge or reducing the thermal loading of semiconductors.

The experiments demonstrate that the RMS current of grid-connected bricks can be reduced to 32.1 A, a reduction of 40 % with respect to other strategies. This impacts the electrical departure ratings and can have significant cost impact in large industrial installations. Similarly the energy storage utilisation can can be as much as 25% lower at 37.7 kJ when the relevant strategy is employed. This improvement implies a possible cost saving if lower energy storing capacity is used in the bricks. Finally, the peak brick current can also be optimised for selected bricks by lowering the output current to 373.2 A from 444.3 A and this has an impact on the choice of the switching device ratings as well as in the cooling requirements.

REFERENCES

1. Kumar KN, Miskiewicz R, Trochimiuk P, Rabkowski J, Peftitsis D. Performance Evaluation of SiC-based Isolated Bidirectional DC/DC Converters for Electric Vehicle Charging. 2022 24th European Conference on Power Electronics and Applications (EPE'22 ECCE Europe). 2022;p. 11.
2. Vermulst BJD, Duarte JL, Lomonova EA, Wijnands KGE. Scalable multiport active-bridge converters: Modelling and optimised control. IET Power Electronics. 2017;10(1):80–91.
3. Galeshi S, Frey D, Lembeye Y. Efficient and scalable power control in multiport active-bridge converters. 2020 22nd European Conference on Power Electronics and Applications, EPE 2020 ECCE Europe. 2020;p. 2–10. ISBN: 9789075815368.
4. Peng P, Li Y, Li Z, Shao Y, Luo X, Wang Y, et al. Analysis of Advantage of the Connection of Energy Storage System to Distribution Network and the Impact on the Voltage Quality. In: 2nd IEEE Conference on Energy Internet and Energy System Integration, EI2 2018 - Proceedings. 1; 2018. p. 2018–2021. Publisher: IEEE ISBN: 9781538685495.
5. Parchomiuk M, Strzelecki R, Zymmer K, Domino A. Modular power converter topologies for energy storage and electric power distribution systems. 2017 Progress in Applied Electrical Engineering, PAEE 2017. 2017;ISBN: 9781538615287.
6. Ould Amrouche S, Rekioua D, Rekioua T, Bacha S. Overview of energy storage in renewable energy systems. International Journal of Hydrogen Energy. 2016;41(45):20914–20927. Publisher: IEEE ISBN: 9781467378949.
7. Brown DR, Chvala WD. Flywheel energy storage: An alternative to batteries for ups systems. Energy Engineering: Journal of the Association of Energy Engineering. 2005;102(5):7–26.
8. Magdalena Stephan R, de Andrade Jr R, Gonçalves Sotelo G. Third Generation Of Flywheels: A Promising Substitute To Batteries. Eletrônica de Potência. 2008;13(3):171–176.
9. Wang G, Konstantinou G, Townsend CD, Pou J, Vazquez S, Demetriades GD, et al. A review of power electronics for grid connection of utility-scale battery energy storage systems. IEEE Transactions on Sustainable Energy. 2016 Oct;7(4):1778–1790. Available from: http://ieeexplore.ieee.org/document/7506096/.
10. Ise T, Kita M, Taguchi A. A hybrid energy storage with a SMES and secondary battery. IEEE Transactions on Applied Superconductivity. 2005;15(2 PART II):1915–1918.
11. Ängquist L, Antonopoulos A, Siemaszko D, Ilves K, Vasiladiotis M, Nee HP. Open-loop control of modular multilevel converters using estimation of stored energy. IEEE Transactions on Industry Applications. 2011;47(6):2516–2524.
12. Ilves K, Harnefors L, Norrga S, Nee HP. Analysis and operation of modular multilevel converters with phase-shifted carrier PWM. IEEE Transactions on Power Electronics. 2015;30(1):268–283.
13. Perez MA, Bernet S, Rodriguez J, Kouro S, Lizana R. Circuit topologies, modeling, control schemes, and applications of modular multilevel converters. IEEE Transactions on Power Electronics. 2015 Jan;30(1):4–17. Available from: http://ieeexplore.ieee.org/lpdocs/epic03/wrapper.htm?arnumber=6757004.
14. Rodal GL, Acharya AB, Norum LE. Analysis and Evaluation of Repetitive Controllers for Circulating Current Suppression in Modular Multilevel Converters. 2018 20th European Conference on Power Electronics and Applications, EPE 2018 ECCE Europe. 2018;p. 1–10. ISBN: 9789075815283.
15. Carrasco JM, Franquelo LG, Bialasiewicz JT, Galvan E, Portillo Guisado RC, Prats MAM, et al. Power-electronic systems for the grid integration of renewable energy sources: A survey. IEEE Transactions on Industrial Electronics. 2006;53(4):1002–1016.
16. Errigo F, Chedot L, Morel F, Venet P, Sari A. Modelling and Control of an MMC-HVDC Submodule with Energy Storage for Fast Frequency Response. 2021 23rd European Conference on Power Electronics and Applications, EPE 2021 ECCE Europe. 2021;ISBN: 9789075815375.
17. Vasiladiotis M, Rufer A. Analysis and control of modular multilevel converters with integrated battery energy storage. IEEE Transactions on Power Electronics. 2015;30(1):163–175. Publisher: IEEE.
18. Batarseh I, Alluhaybi K. Emerging Opportunities in Distributed Power Electronics and Battery Integration: Setting the Stage for an Energy Storage Revolution. IEEE Power Electronics Magazine. 2020;7(2):22–32.
19. Milovanovic S, Strobl S, Ladoux P, Dujic D. Hardware-in-the-Loop Modeling of an Actively Fed MVDC Railway Systems of the Future. IEEE Access. 2021;9:151493–151506.
20. Lamaille BLM, Dragoni F, Evrard S, Harden FJ, Harrouch E, Lazzaroni M, et al. Study of the Energy Savings Resulting From the East Area Renovation. 10th Int Partile Accelerator Conferance. 2019;p. 4023–4025. ISBN: 9783954502080.
21. Maestri S, Retegui RG, Carrica D, Rossini S, Le Godec G, Papastergiou K. Figures of merit for the evaluation of regenerative power converters. 2016 18th European Conference on Power Electronics and Applications, EPE 2016 ECCE Europe. 2016;p. 1–9. Publisher: Jointly owned by IEEE-PELS and EPE Association ISBN: 9789075815245.
22. Parchomiuk M, Strzelecki R, Zymmer K, Sak T. Modular high precision high current source for special applications-Simulation and verification. Proceedings - 2016 10th International Conference on Compatibility, Power Electronics and Power Engineering, CPE-POWERENG 2016. 2016;p. 422–427. Publisher: IEEE ISBN: 9781467372930.
23. Asimakopoulos P, Papastergiou K, Thiringer T, Bongiorno M, Le Godec G. On Vce Method: In Situ Temperature Estimation and Aging Detection of High-Current IGBT Modules Used in Magnet Power Supplies for Particle Accelerators. IEEE Transactions on Industrial Electronics. 2019;66(1):551–560.
24. Boukettaya G, Krichen L. A dynamic power management strategy of a grid connected hybrid generation system using wind, photovoltaic and Flywheel Energy Storage System in residential applications. Energy. 2014 Jul;71:148–159. Publisher: Pergamon. Available from: https://www.sciencedirect.com/science/article/pii/S0360544214004526.
25. Dekka A, Wu B, Fuentes RL, Perez M, Zargari NR. Evolution of Topologies, Modeling, Control Schemes, and Applications of Modular Multilevel Converters. IEEE Journal of Emerging and Selected Topics in Power Electronics. 2017;5(4):1631–1656.
26. Lesnicar A, Marquardt R. An innovative modular multilevel converter topology suitable for a wide power range. 2003 IEEE Bologna PowerTech - Conference Proceedings. 2003;3:272–277. ISBN: 0780379675.
27. Haugen KL, Papastergiou K, Asimakopoulos P, Peftitsis D. Energy flow control in a modular DC-DC converter with energy recovery. In: 2021 IEEE 12th International Symposium on Power Electronics for Distributed Generation Systems (PEDG). Chicago, IL, USA: IEEE; 2021. p. 1–8. Available from: https://ieeexplore.ieee.org/document/9494229/.
28. Wang C, Li X, Peng H, He L, Xue Y. Segmented Energy Routing for a Modular AC/DC Hybrid System. IEEE Journal of Emerging and Selected Topics in Power Electronics. 2021;6777(c):1–1. Publisher: IEEE.
29. Ma F, Wang X, Deng L, Zhu Z, Xu Q, Xie N. Multiport Railway Power Conditioner and Its Management Control Strategy with Renewable Energy Access. IEEE Journal of Emerging and Selected Topics in Power Electronics. 2020;8(2):1405–1418. Publisher: IEEE.
30. Zhang Z, Jin C, Tang Y, Dong C, Lin P, Mi Y, et al. A Modulized Three-Port Interlinking Converter for Hybrid AC/DC/DS Microgrids Featured with a Decentralized Power Management Strategy. IEEE Transactions on

Industrial Electronics. 2021;68(12):12430–12440. Publisher: IEEE.
31. De Castro R, Pereira H, Araujo RE, Barreras JV, Pangborn HC. *qTSL* : A Multilayer Control Framework for Managing Capacity, Temperature, Stress, and Losses in Hybrid Balancing Systems. IEEE Transactions on Control Systems Technology. 2022 May;30(3):1228–1243. Available from: https://ieeexplore.ieee.org/document/9520124/.
32. Haugen KL, Papastergiou K, Peftitsis D. A scalable DC/DC converter topology with modularised energy storage for high energy physics applications. IEEE Journal of Emerging and Selected Topics in Power Electronics. 2023;p. 1–1. Available from: https://ieeexplore.ieee.org/document/10105646/.
33. Haugen KL, Papastergiou K, Asimakopoulos P, Peftitsis D. On dimensioning the fundamental brick for a scalable DC-DC converter with energy recovery. In: 2021 23rd European Conference on Power Electronics and Applications (EPE'21 ECCE Europe). Ghent, Belgium: IEEE; 2021. p. P.1–P.10. Available from: https://ieeexplore.ieee.org/document/9570676/.
34. Haugen KL, Papastergiou K, Asimakopoulos P, Peftitsis D. High precision scalable power converter for accelerator magnets. Journal of Instrumentation. 2022 Mar;17(03):C03021. Available from: https://iopscience.iop.org/article/10.1088/1748-0221/17/03/C03021.
35. Kish GJ. On the emerging class of non-isolated modular multilevel DC-DC converters for DC and hybrid AC-DC systems. IEEE Transactions on Smart Grid. 2019;10(2):1762–1771. Publisher: IEEE.
36. Goetz SM, Peterchev AV, Weyh T. Modular multilevel converter with series and parallel module connectivity: Topology and control. IEEE Transactions on Power Electronics. 2015 Jan;30(1):203–215. Publisher: IEEE.
37. Masaud TM, Lee K, Sen PK. An overview of energy storage technologies in electric power systems: What is the future? North American Power Symposium 2010, NAPS 2010. 2010;Publisher: IEEE ISBN: 9781424480463.